Materials Letters 188 (2017) 304–307

Contents lists available at ScienceDirect

Materials Letters

journal homepage: www.elsevier.com/locate/matlet

N-doped carbon quantum dots/Ag_3PO_4 hybrid materials with improved visible light photocatalytic activity and stability

Chaosheng Zhu, Yuanyuan Zhao, Liyang Fang, Jingtang Zheng*, Ping Hu, Yukun Liu, Xiaoqing Cao, Zhenzhen Chen, Wenting Wu, Mingbo Wu*

State Key Laboratory of Heavy Oil Processing, China University of Petroleum, Qingdao 266580, Shandong, PR China

ARTICLE INFO

Keywords:
Carbon materials
Nanocomposites
N-CQDs
Photocatalysts
Ag_3PO_4

ABSTRACT

In this study, the N-doped carbon quantum dots (N-CQDs) were applied to combine with Ag_3PO_4 and form N-CQDs/Ag_3PO_4 hybrid materials with improved photocatalytic activity and stability toward organic dyes degradation under visible light irradiation. The efficiency of 2%N-CQDs/Ag_3PO_4 is improved by 20.8% higher than that of pure Ag_3PO_4 for the degradation MB and is retained fairly high levels after 4 successive recycling experiments. The improved photocatalytic activity and superior cycle performance are mainly ascribed to the N-CQDs as the electron acceptor enhanced the spatial separation of photogenerated charge carriers and inhibited the reduction of silver ions.

1. Introduction

As a new member of carbon quantum dots family, the N-doped CQDs have intrigued scientists because they are characterized by low toxicity, biocompatibility, and good photoinduced electron transfer ability [1]. Recently, in the photocatalytic environment purification field, N-CQDs have also come to arouse some interest and attention from researchers, but not seemingly enough [2,3].

Of the well-known photocatalysts, silver orthophosphate (Ag_3PO_4) has super photooxidative capabilities under visible light irradiation [4]. However, identity challenges encountered by almost photocatalysts are hanging over Ag_3PO_4, for instance, the rapid recombination of electron–hole pairs [5]. In addition, Ag_3PO_4 is slightly soluble in aqueous solution and susceptible to corrosion under prolonged light illumination due to the existence of photogenerated electrons [6]. Many elaboration work has demonstrated that coupling Ag_3PO_4 with carbon-based materials was an effective way to solve these intractable problems [7–10]. However, to the best of our knowledge, despite the many advantages, no work has been published on coupling with N-CQDs to improve the photocatalytic activity and stability of Ag_3PO_4.

In this study, N-CQDs/Ag_3PO_4 hybrid materials were first prepared through a simple low temperature chemical precipitation method. The structures, morphologies and optical properties were investigated in detail by XRD, HRTEM, XPS, UV–vis DRS and PL analysis. The photocatalytic properties and stabilities of composites were evaluated and the reaction mechanism of increased photocatalytic activity was also discussed.

2. Experimental

2.1. Synthesis of N-CQDs/Ag_3PO_4 composites

N-CQDs were synthesized via facile and one-step hydrothermal approach from soy flour with NaOH assisted reaction (see support materials). The N-CQDs/Ag_3PO_4 nanocomposites were prepared by a simple deposition–precipitation process. Firstly, a certain amount of N-CQDs and 0.5g PVP were suspended in 50 mL distilled water, followed by the addition of 0.2g $AgNO_3$ and required amount of Na_2HPO_4 solution (0.03 M) under stirring. The mixture solution was stirred for 4 h under dark condition and centrifuged at 5000 rpm. The obtained products were washed several times with distilled water and absolute ethyl alcohol and dried at 60 °C for 12 h. For comparison, Ag_3PO_4 was likewise synthesized by the similar method without addition of N-CQDs.

2.2. Characterization of the as-prepared photocatalysts

The as-prepared photocatalysts were characterized by TEM (JEM-2100UHR), FT-IR (FTS-3000), Raman spectroscopy (HR 800), XRD (PANalytical B.V.), XPS (PHI 5000 C ESCA), UV–Vis spectrometer (UV-2450) and PL spectra (Hitachi F-4500, excitation wavelength 210 nm).

* Corresponding authors.
E-mail addresses: jtzheng03@163.com (J. Zheng), wumb@upc.edu.cn (M. Wu).

http://dx.doi.org/10.1016/j.matlet.2016.10.105
Received 23 June 2016Received in revised form 19 October 2016Accepted 25 October 2016
Available online 28 October 2016
0167-577X/

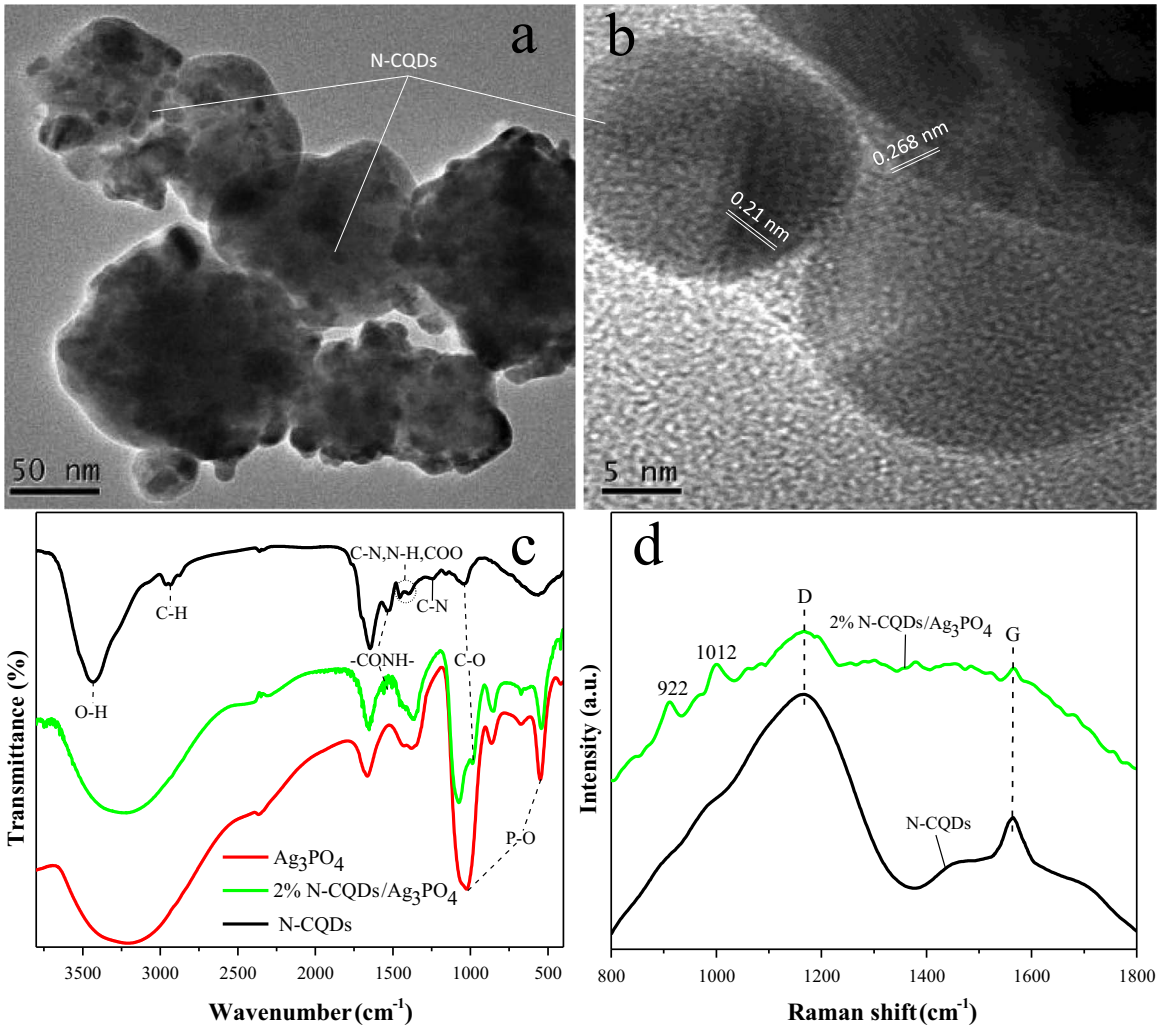

Fig. 1. TEM image (a) and HRTEM image (b) of 2%N-CQDs/Ag_3PO_4. FT-IR spectra (c) and Raman spectrum (d) of the as-prepared samples.

2.3. Photocatalytic performance measurements

A series of cylindrical quartz photoreactors with a volume of 80 mL were used, inside which a 300 W Xe arc lamp with a 420 nm optical filter was positioned as the visible-light source. 50 mg photocatalyst was ultrasonically dispersed in 50 mL of MB aqueous solution (20 mg L^{-1}) for 10 min and then stirred in the dark for 60 min to reach the adsorption–desorption equilibrium. The decolorization ratio of MB was evaluated by measuring the absorbance of the reaction liquid at 10 min interval.

3. Results and discussion

3.1. Character of photocatalysts synthesized

The microstructures of the N-CQDs/Ag_3PO_4 composites were observed by TEM (Fig. 1a). It is clearly ascertained that the N-CQDs are well-dispersed on the surface of Ag_3PO_4 nanoparticles. HRTEM image (Fig. 1b) clearly displays the resolved lattice fringes of 0.21 nm and 0.268 nm, which corresponds to the (100) diffraction facet of graphite carbon and (210) planes of cubic phase of Ag_3PO_4, respectively [11,12]. It clearly reveals that the N-CQDs have been coupled with Ag_3PO_4 in the nanoscale successfully.

Fig. 1c shows the typical FT-IR spectrums of the as-prepared samples. In the FT-IR spectrum of 2%N-CQDs/Ag_3PO_4, both the partial absorption peaks of N-CQDs and the typical absorption peaks of Ag_3PO_4 were observed. The characteristic peaks' intensity of composites is weaker than one component, which indicates a possibility of compounding between N-CQDs and Ag_3PO_4. Two characteristic peaks are observed in the Raman spectra of 2%N-CQDs/Ag_3PO_4 and N-CQDs, corresponding to the D-band and G-band of carbon, respectively (Fig. 1d). The D-band centers at 1191 cm^{-1} arise from the extent of defects of sp3 carbon atoms and the G-band at 1565 cm^{-1} is attributed to the sp2 carbon atoms [13].

The XRD patterns of N-CQDs, Ag_3PO_4 and N-CQDs/Ag_3PO_4 composites are shown in Fig. 2a. In the pattern of the pure N-CQDs, a broader and low-intensity diffraction peak centers at 2θ=20.12°, which reveals a graphite carbon phase [10]. As for Ag_3PO_4, all of the diffraction peaks can be clearly assigned to the cubic phase of Ag_3PO_4 (JCPDS card no. 06-0505) [14]. It can be seen that N-CQDs/Ag_3PO_4 composites exhibit similar XRD patterns to Ag_3PO_4 and no diffraction peaks of N-CQDs were found is owing to the fact that the tiny of highly dispersed N-CQDs cannot be resolved by XRD. Fig. 2b displays the full XPS spectrum of the 2%N-CQDs/Ag_3PO_4. The photoelectron peaks of O1s, N1s, C1s, P2p and Ag peaks are clearly observed, which indicates that the N-CQDs exist in the composites.

The UV–vis absorption spectra of Ag_3PO_4 and 2%N-CQDs/Ag_3PO_4 is shown in Fig. 2c. The Ag_3PO_4 shows a sharp fundamental absorption edge at about 530 nm, which falls in with other reports [15]. An evident red-shift of photo-absorption edge was observed in the UV–vis absorption spectrum of 2%N-CQDs/Ag_3PO_4 which indicates the enhanced visible absorption. The wider absorption edge indicates that the

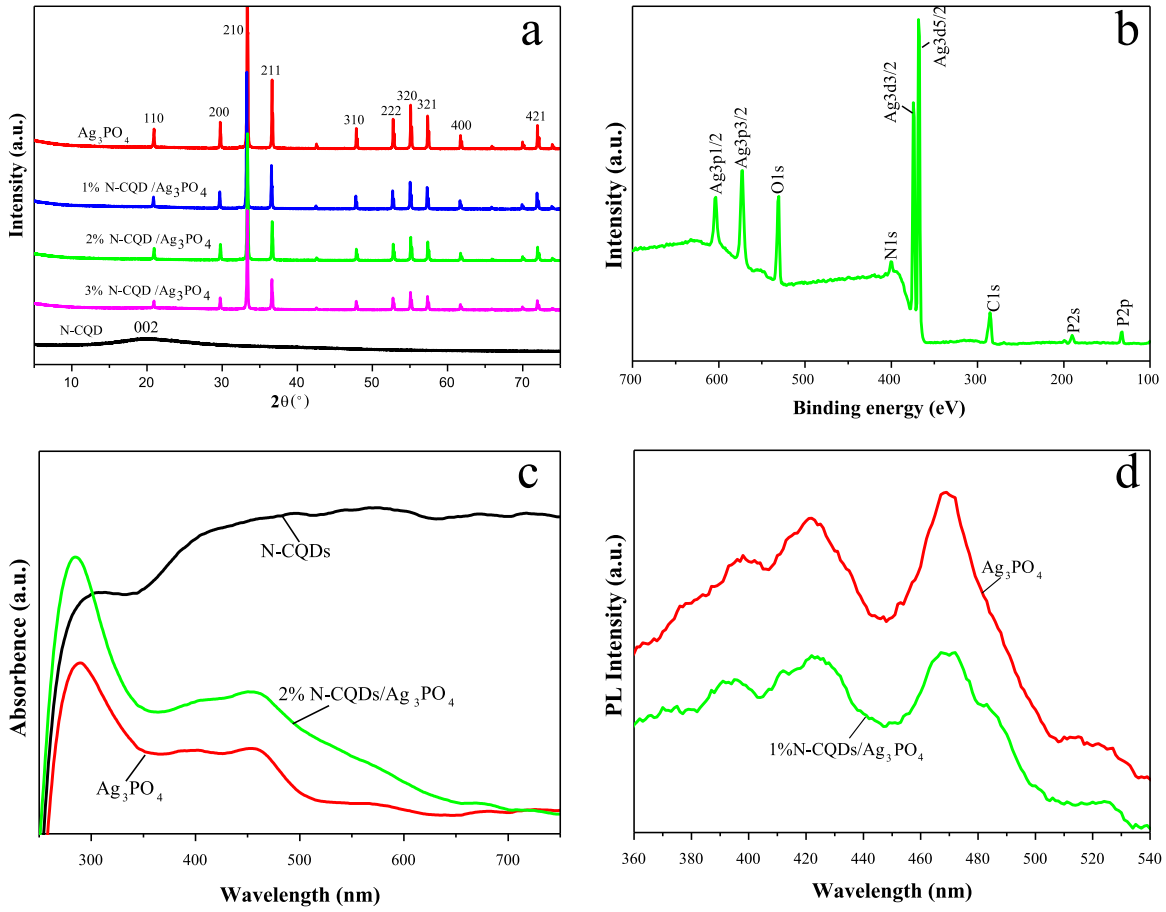

Fig. 2. XRD pattern (a), survey XPS spectrum (b), UV–vis diffuse reflection spectra (c) and PL spectra (d) of the as-prepared samples.

N-CQDs/Ag_3PO_4 composites have greater carrier concentration, which can be favorable for photocatalytic reactions. Fig. 2d shows the PL spectra for Ag_3PO_4 sample as well as 2%N-CQDs/Ag_3PO_4. They all exhibited a main emission peak centered at around 465 nm. However, the emission intensity of 2%N-CQDs/Ag_3PO_4 is visibly reduced compared with that of Ag_3PO_4, indicating that the recombination of the photoexcited charge carriers is suppressed in the N-CQDs/Ag_3PO_4 composite photocatalysts.

3.2. Photocatalytic performance of samples synthesized

The photocatalytic activities of the as-prepared samples are provided in Fig. 3a. In comparison with Ag_3PO_4, the N-CQDs/Ag_3PO_4 composites exhibit superior photocatalytic activities and the N-CQDs content plays a key role on their photocatalytic performance. The 2%N-CQDs/Ag_3PO_4 can nearly completely decolorize 20 mg L^{-1} MB within 70 min of visible-light irradiation while the Ag_3PO_4 can only decompose 78.8% of MB during the same interval. The first-order kinetic behaviors of as-prepared samples for photodegradation of MB were plotted in Fig. 3b, there is a nice linear correlation between $\ln(C/C_O)$ and the reaction time (t). According to the photocatalytic performance, the optimal sample is 2%N-CQDs/Ag_3PO_4 and its apparent rate constants value for MB degradation is about 1.95 times of Ag_3PO_4.

As is shown in Fig. 3c, the bleaching efficiency of Ag_3PO_4 shows a greatly reduction during the repeated photocatalytic reactions and decreases by 47.8% after 4 successive cycling runs, but the photocatalytic decoloration rate of the 2%N-CQDs/Ag_3PO_4 does not show major loss, which indicates that the N-CQDs/Ag_3PO_4 composite photocatalysts possess good reusability. The metallic Ag nanoparticles maybe produce from the photocorrosion of Ag_3PO_4 under the visible-light irradiation and the Ag nanoparticles on the surface of photocatalyst cause a light shielding effect and inhibit the transfer of holes between photocatalyst and solution. Therefore, the photocatalytic activity of as-prepared samples decreased gradually with increasing the cycling runs. The high photocatalytic stability of the N-CQDs/Ag_3PO_4 coupled system is due to the reduction of silver ions which is effectively inhibited by carrying the photogenerated electrons of Ag_3PO_4 to the N-CQDs. And beyond that, the N-CQDs are in firmly contact with the surface of the Ag_3PO_4, to some extent, reducing the dissolution of the Ag_3PO_4.

On the basis of the above mentioned for the N-CQDs/Ag_3PO_4 composite photocatalysts, the photocatalytic mechanism is tentatively proposed and schematically illustrated in Fig. 3d. Ag_3PO_4 can be easily excited to yield photon-generated carriers under visible-light irradiation, and photoinduced electrons from the VB are transferred to the corresponding CB, leaving the holes in the VB. As for Ag_3PO_4, the large numbers of electron–hole pairs are prone to recombine. Nevertheless, after N-CQDs are intermingled, the photo-generated electrons are effectual trapped by N-CQDs and further reduce the adsorbed O_2 to $\bullet O_2^-$. The holes of the VB of Ag_3PO_4 would photocatalytic oxidize MB directly and the high reducing electron of the CB of N-CQDs would react with O_2 to form $\bullet O_2^-$, which can further oxidize MB [16]. Therefore, the efficient photodegradation progress of MB can smoothly proceed. According to the above-mentioned charge-carrier transfer process, the photogenerated carriers are spatially separated and their lifetime can be significant improved for N-CQDs/Ag_3PO_4 composites which bring about superior photocatalytic activity and stability.

4. Conclusions

A series of N-CQDs/Ag_3PO_4 composite photocatalysts with different N-CQDs content were facilely prepared and used for MB dye degrada-

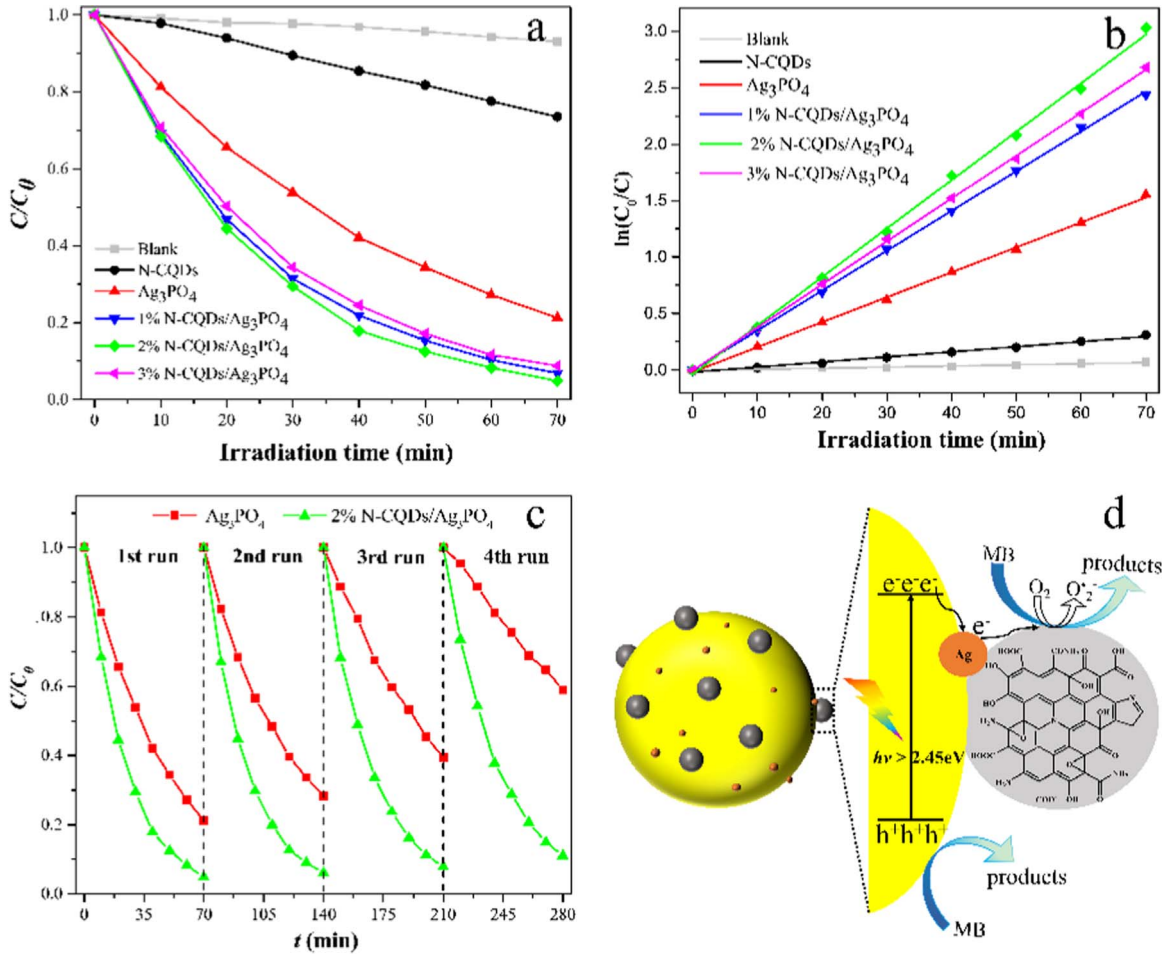

Fig. 3. Photocatalytic degradation (a), pseudo-first-order kinetics rates (b) and repeated photocatalytic experiments (c) of obtained photocatalyst for degradation of MB. Schematic of photocatalytic mechanism of N-CQDs/Ag_3PO_4 hybrid materials (d).

tion under visible light illumination. The composite samples exhibited outstanding photocatalytic activity and stability due to the fact that the introduction of N-CQDs significantly improves the separation of photogenerated charge carriers. On the basis of the results of this study, the N-CQDs/Ag_3PO_4 composite is expected to be a promising visible-light photocatalyst for environment purification field.

Acknowledgments

This work is financially supported by the National Natural Science Foundation of China (Nos. 21376268 and 51372277), Fundamental Research Funds for the Central Universities (Nos. 15CX08005A and 15CX06050A) and Graduate Innovation Project of China University of Petroleum (No. YCXJ2016055).

Appendix A. Supplementary material

Supplementary data associated with this article can be found in the online version at http://dx.doi.org/10.1016/j.matlet.2016.10.105.

References

[1] A. Cayuela, C. Carrillo-Carrión, M.L. Soriano, Anal. Chem. 88 (2016) 3178–3185.
[2] J. Zhang, X. Zhang, S. Dong, J. Photochem. Photobiol. A 325 (2016) 104–110.
[3] N.C.T. Martins, J. Ângelo, A.V. Girão, T. Trindade, Appl. Catal. B 193 (2016) 67–74.
[4] Z. Hao, L. Ai, C. Zhang, Mater. Lett. 143 (2015) 51–54.
[5] X. Lin, X. Guo, W. Shi, Catal. Commun. 71 (2015) 21–27.
[6] D.J. Martin, G. Liu, S.J. Moniz, J. Tang, Chem. Soc. Rev. 44 (2015) 7808–7828.
[7] T. Liu, Y. Dai, X. Chen, Mater. Lett. 161 (2015) 678–681.
[8] H. Cui, X. Yang, Q. Gao, Mater. Lett. 93 (2013) 28–31.
[9] B. Liu, Z. Li, S. Xu, T. Cong, Mater. Lett. 131 (2014) 229–232.
[10] H. Zhang, H. Huang, H. Ming, J. Mater. Chem. 22 (2012) 10501–10506.
[11] X. Guo, C. Wang, Z. Yu, L. Chen, Chem. Commun. 48 (2012) 2692–2694.
[12] C. Tang, E. Liu, J. Wan, Appl. Catal. B 181 (2016) 707–715.
[13] Y. Hu, J. Yang, J. Tian, Carbon 77 (2014) 775–782.
[14] Y. Song, Y. Lei, H. Xu, C. Wang, J. Yan, H. Zhao, Dalton Trans. 44 (2015) 3057–3066.
[15] Z. Chen, W. Wang, Z. Zhang, X. Fang, J. Phys. Chem. C 117 (2013) 19346–19352.
[16] X. Lin, J. Hou, X. Guo, Sep. Purif. Technol. 156 (2015) 875–880.